

## Characterization and Ionic Conductivity Studies on Nano SiO<sub>2</sub> Dispersed x NaNO<sub>3</sub>-(1-x) Sr(NO<sub>3</sub>)<sub>2</sub> Mixed System.

S Narender Reddy\*

Department of Physics, University College of Engineering, Osmania University, Hyderabad, Andhra Pradesh, India.

### Research Article

Received: 17/08/2013

Revised: 17/09/2013

Accepted: 25/09/2013

#### \*For Correspondence

Department of Physics,  
University College of  
Engineering, Osmania University,  
Hyderabad, Andhra Pradesh,  
India.

Mobile: +91 9949055469

**Keywords:** Dispersed Solid  
electrolyte, Superionic  
conductor, Enhancement, Ionic  
conductivity.

#### ABSTRACT

Variation of dc ionic conductivity with temperature and mole percent in dispersed mixed ionic conductors of Sodium and Strontium nitrates is presented. The host materials, mixed systems of NaNO<sub>3</sub> and Sr(NO<sub>3</sub>)<sub>2</sub> single crystals were grown by solution technique. The powders of different compositions of mixed systems were prepared and then dispersed with SiO<sub>2</sub> (10nm) in a particular mole percent. Pellets were made at a pressure of about 5tonnes/sq.m. and sintered at 250°C for 20hours. The room temperature X-ray diffraction patterns of dispersed systems show the co-existence of three phases. The Fourier Transform Infrared spectrum of dispersed systems in the wave number range from 400 to 4000 cm<sup>-1</sup> show the existence of three phases and also confirms the existence of OH<sup>-</sup> band. In the dispersed systems the enhancement in conductivity is observed to increase with mole percent (m/o) with a threshold at 20.55 m/o where from enhancement starts falling with further increase in mole percent. The maximum enhancement at 20.55 m/o is observed to be above two orders of magnitude with respect to mixed system in the extrinsic conduction region. The enhancement of conductivity in these systems is explained using Maier's space charge model. The enhancement of conductivity in the dispersed systems is mainly attributed to the increased concentration defects in the space charge layer formed between the host material and the dispersoid. Further, the fall in conductivity may be due to the fall of total effective surface area of contact between the host and dispersoid materials.

#### INTRODUCTION

In recent years there has been much interest in materials which show high ionic conductivity at ambient temperatures, because their potential applications in various electrochemical devices such as, solid-state batteries, sensors, fuel cells etc [1]. There exist many solids with high ionic conductivity (> 10<sup>-4</sup> S/m) and negligible electronic conductivity (<10<sup>-12</sup> S/m) which are referred as fast ion conductors. One of the most important applications of superionic conductors is, as electrolyte in batteries and hence, often, they are also called as solid electrolytes. There are many advantages in electrochemical devices using solid electrolytes instead of liquid electrolytes namely: longer life, high energy density, compact power batteries which are used in pacemakers and mobile telephones and laptops and no possibility of leakage current etc. Various solids with high ionic conductivity, such as Ag<sub>3</sub>SI and RbAg<sub>4</sub>I<sub>5</sub> were discovered in 1960s [2, 3]. The discovery of β-alumina, an excellent solid electrolyte in 1967 by Yao and Kummer and used successfully in battery cells boosted the research in the framed structures [4]. The synthesis and characterization studies on Li ion conductors are motivated by its small ionic radii of Li<sup>+</sup>, lower weight, ease of handling and potential use in high energy storage batteries [5,6,7,8]. Though the above are of crystalline but many of the superionic solids of glassy in nature [9,10,11] as well as polymer based [12,13,14,15] and also dispersed solid electrolytes [16,17,18,19] are also being studied extensively. The dispersion of second phase particles into host ionic material is one among several approaches to increase the ionic conductivity of solid electrolytes. In the present study we have chosen the mixed system of a particular composition, where in the maximum conductivity is recorded among all, as a host ionic solid in which the SiO<sub>2</sub> is used as dispersed second phase particle and presented the results of variation of conductivity with temperature and mole percent of dispersoid SiO<sub>2</sub>.

## EXPERIMENTAL

The host materials, (85.32)  $\text{NaNO}_3$  - (14.68)  $\text{Sr}(\text{NO}_3)_2$  single crystals, were grown by solution technique using analar grade BDH chemicals of 99.5 purity. The powders of mixed systems were prepared by grinding the single crystals for several hours to obtain fine powder and sieved with No.300 mesh, then dispersed with  $\text{SiO}_2$  (10nm) in 7.94, 14.71, 20.55, 25.64 and 30.12 mole percentages by mixing them mechanically in the presence of acetone until the uniformity is obtained in the powder. These powders were made pellets by applying a pressure of about 5tonnes/sq.m. and sintered them at 250°C for 20 hours. These pellets were polished smoothly and applied silver paint on either flat faces and these were mounted between the electrodes of the sample holder for conductivity studies. A small dc voltage of 1V was applied across the sample and the current was recorded by Agilent electrometer. The small amount of well grounded powder was used for XRD and FTIR analyses.

## RESULTS AND DISCUSSION

### X-ray Diffraction (XRD)

Figure 1 shows XRD patterns, of pure mixed system  $[\text{NaNO}_3]_{(1-x)}[\text{Sr}(\text{NO}_3)_2]_x$   $x = 14.68$ ,  $\text{SiO}_2$  and dispersed with different mole percent of  $\text{SiO}_2$  systems, recorded at room temperature by using Regaku miniflex diffractometer. It is observed from the figure that the pure mixed system has distinct peaks indicating that it is in the crystalline form and XRD pattern of pure  $\text{SiO}_2$  shows that broad prominent peaks along with intense background pattern indicates that the size of  $\text{SiO}_2$  particles is in the order of nanometers. It can be noticed from the Fig.1 that XRD peaks of the composite systems move to lower diffraction angles and become broader with respect to pure mixed system. This indicates that the average crystallite size of ionic salt decreases due the spreading of ionic salt along a large surface of the dispersoid. No additional peaks have been noticed in the patterns of dispersed compositions signifies that there is chemical reaction or the formation of solid solution between the host material and dispersoid  $\text{SiO}_2$ . It also reveals that the phases of the parent compounds exist separately, i.e. the samples remain in multiphase mixture of  $\text{NaNO}_3$ ,  $\text{Sr}(\text{NO}_3)_2$  and  $\text{SiO}_2$  [20,21,23].

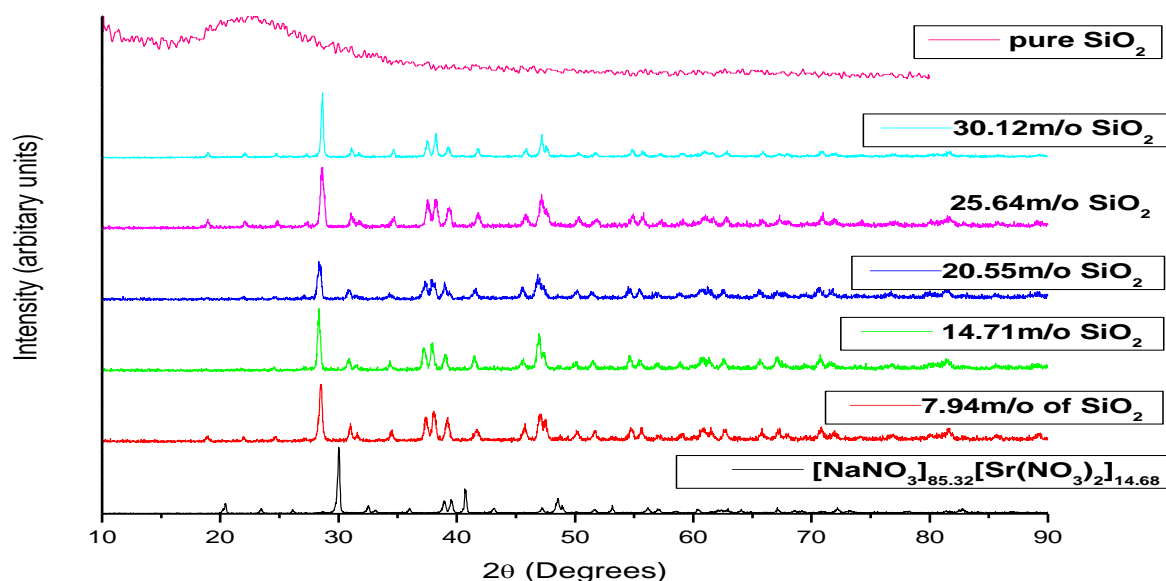


**Figure 1:** X-ray diffraction patterns of the pure mixed system  $[\text{NaNO}_3]_{(1-x)}[\text{Sr}(\text{NO}_3)_2]_x$   $x = 14.68$ , pure  $\text{SiO}_2$  and dispersed systems of different m/o of  $\text{SiO}_2$  systems.

### Fourier Transform Infrared Spectroscopy (FTIR)

Figure 2 shows the FTIR spectra of the pure mixed system,  $\text{SiO}_2$  and dispersed systems of different m/o of  $\text{SiO}_2$  in the wave number range from 400 to 4000  $\text{cm}^{-1}$ . It can be observed from the figure that sharp peaks at 735  $\text{cm}^{-1}$ , 835  $\text{cm}^{-1}$  and 1385  $\text{cm}^{-1}$  in pure mixed system. The sharp peak observed at 835  $\text{cm}^{-1}$  is due to the vibration of N in and out of  $\text{NO}_3$  plane and the strongest absorption at 1385  $\text{cm}^{-1}$  due to asymmetric  $\text{NO}_3$  stretch which confirms the presence of nitrate [24]. The weak absorption which is observed at 735  $\text{cm}^{-1}$  gives the doubly generate O-N-O bending [25]. In the pure  $\text{SiO}_2$  spectrum broad absorption bands at 468  $\text{cm}^{-1}$ , 800  $\text{cm}^{-1}$  and 1101  $\text{cm}^{-1}$  are attributed to the asymmetric stretching vibration, symmetric stretching vibration and bending vibration of Si-O-Si bond. A broad absorption band around 3420  $\text{cm}^{-1}$  is designated to O-H vibration of the absorbed  $\text{H}_2\text{O}$  [26]. The FTIR

spectrum reveals as much hydroxyl existing as in nano-SiO<sub>2</sub> particles. The presence of other bands corresponding to pure NaNO<sub>3</sub>, Sr(NO<sub>3</sub>)<sub>2</sub> and SiO<sub>2</sub> in the dispersed mixed systems show the existence of three phases independently.

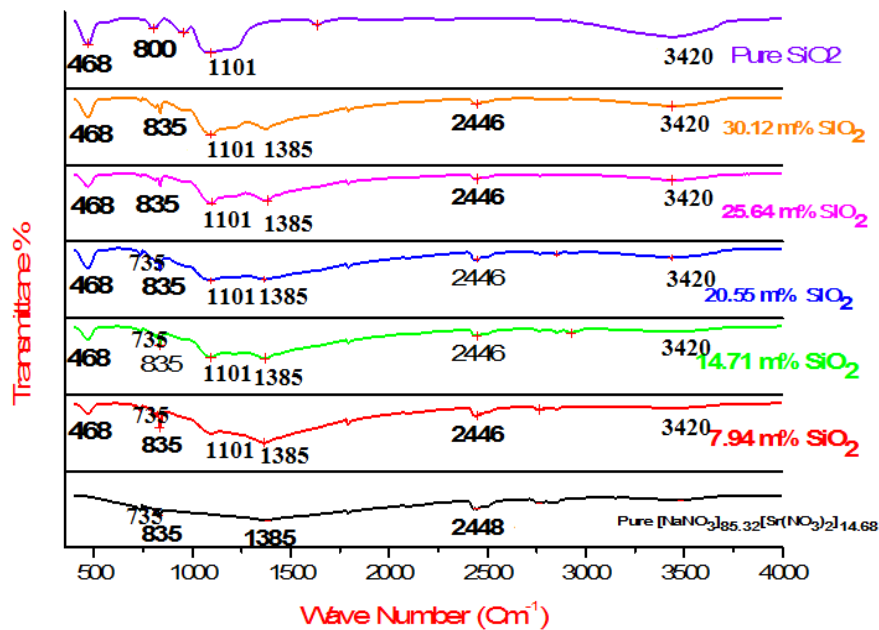


Figure 2: FTIR spectra of the pure mixed system [NaNO<sub>3</sub>]<sub>(1-x)</sub>[Sr(NO<sub>3</sub>)<sub>2</sub>]<sub>x</sub>, pure SiO<sub>2</sub> and dispersed systems of different m/o of SiO<sub>2</sub> systems.

### Differential Scanning Calorimetry (DSC)

DSC curves of the pure mixed system and dispersed systems of different m/o of SiO<sub>2</sub> systems are shown in Figure 3. Pure mixed system exhibits one endothermic peak due to the only transition that a pure NaNO<sub>3</sub> has at 272°C and another peak at 299 °C pertains to the melting point of pure mixed system [27]. As observed from the DSC curves, the SiO<sub>2</sub> content appears to have not affected the transition temperature but showed a slight distortion of the peak toward its low temperature end. The hump which observed here is similar to that in the cases of cesium, rubidium and Sodium nitrate systems. This could be due to the formation of an amorphous phase within the space charge layer that is expected to form between the host material and the dispersoid particles.

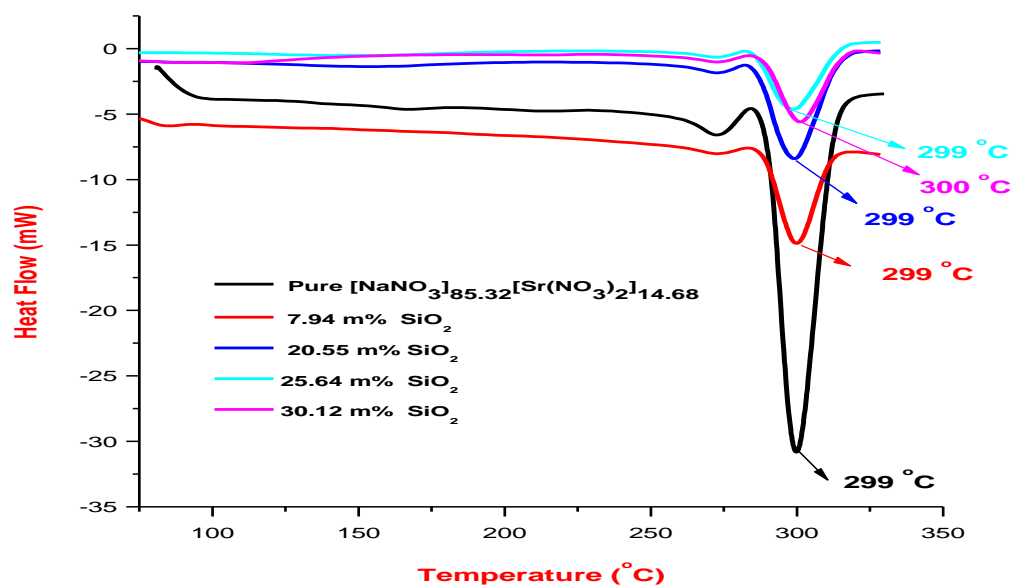


Figure 3: DSC curves of the pure mixed system [NaNO<sub>3</sub>]<sub>(1-x)</sub>[Sr(NO<sub>3</sub>)<sub>2</sub>]<sub>x</sub>, and dispersed systems of different m/o of SiO<sub>2</sub> systems

### Ionic Conductivity

Figure 4 shows the variation of DC ionic conductivity obtained from two-probe dc- technique, with reciprocal temperature in composite systems between room temperature and nearly the transition temperature of the host material for pure mixed and dispersed with different mole percentages of SiO<sub>2</sub> systems. The conductivity in all the samples is, in general noticed to increase with temperature. As we can see from the figure that there is a gradual enhancement in conductivity up to 20.55 m/o of SiO<sub>2</sub> subsequently there is fall of enhancement for 25.64 and 30.12 mole percentages in the extrinsic region of conductivity with respect to pure mixed system. The maximum enhancement in conductivity is noticed to be nearly two orders of magnitude with respect to pure mixed system in the extrinsic region.

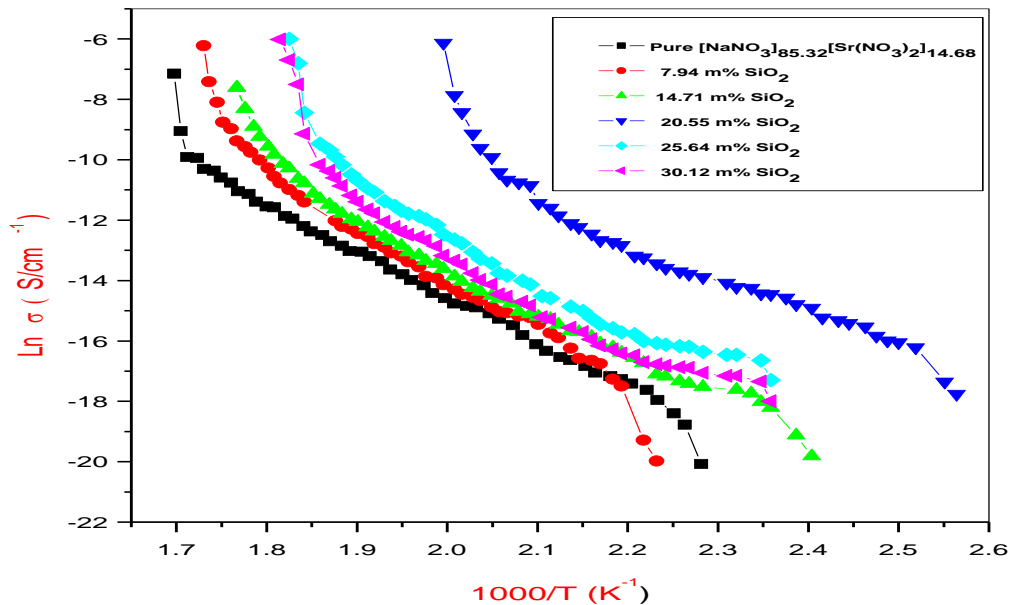


Figure 4: Variation of DC ionic conductivity with reciprocal temperature of the pure mixed system  $[\text{NaNO}_3]_{(1-x)}[\text{Sr}(\text{NO}_3)_2]_x = 14.68$ , and dispersed systems of different m/o of SiO<sub>2</sub>.

The variations of DC ionic conductivity with m/o of SiO<sub>2</sub> plots at different temperatures are shown in figure 5. The enhancement of conductivity in the SiO<sub>2</sub> dispersed composite solid electrolyte systems is observed to increase with mole percent (m/o) and attains maximum at 20.55 m/o, where from enhancement starts falling with further increase in m/o and finally reaches to a lowest value for 30.12.

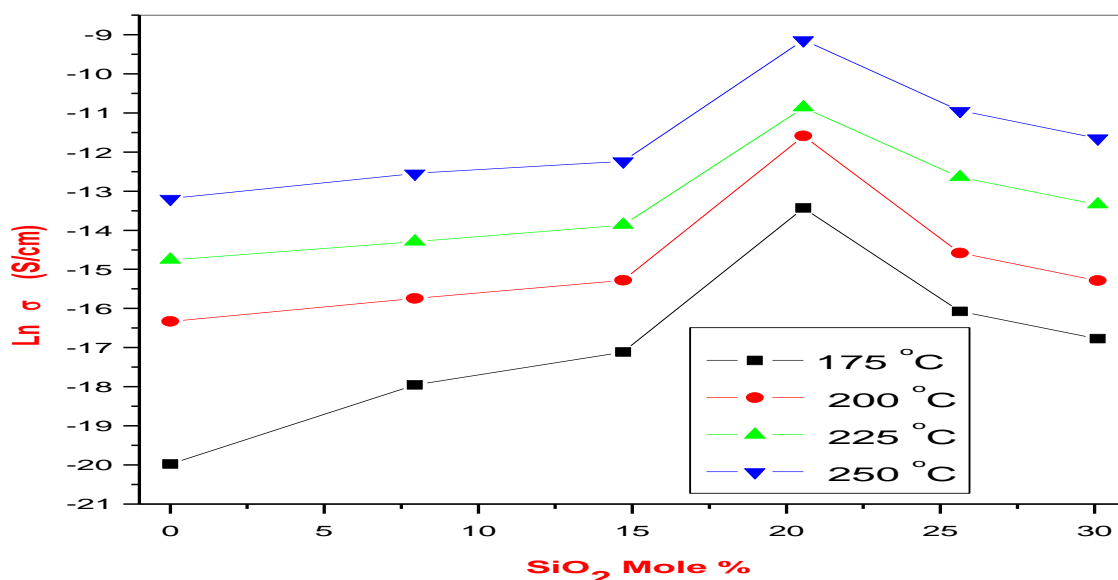


Figure 5: Variation of DC ionic conductivity with m/o of SiO<sub>2</sub>.

Enhanced defect concentration in the space charge layer formed between the host material and the dispersoid is main cause for the enhancement of conductivity. According to the Maier's space charge model the composite solid electrolyte is enriched with defects at the interface of the host and dispersoid due to the surface interaction between the phases of a composite [28,29]. The interfacial interaction between the two phases may be represented as a chemical adsorption of host material (ionic salt) on the dispersoid ( $\text{SiO}_2$ ) surface. The insulating oxide particles can be associated with different hydroxyl groups ( $\text{OH}^-$ ) present on their surfaces. These hydroxyl groups attract the cations into the space charge region as a result, the subsurface region of ionic material enriches in cation vacancies, which describe the subsurface disordering i.e. enhanced defect concentration there by conductivity enhances [29]. The fall of the enhancement of conductivity after reaching the maximum value can be understood as explained as follows. Initially, for low m/o of the dispersoid, the total surface area of contact between the host matrix and the dispersoid particles is small. As the m/o increases, the total surface area in contact increases leading to an increase in the enhancement of conductivity. Further increase of m/o of  $\text{SiO}_2$ , host material is not enough to surround the dispersoid particles individually. This leads to an agglomeration of the particles of the dispersoid leading to a fall of total effective surface area of contact [30, 31].

## CONCLUSIONS

In the dispersed systems the enhancement in conductivity is observed to increase with mole percent (m/o) with a threshold at 20.55 m/o where from enhancement starts falling with further increase in mole percent. The maximum enhancement at 20.55 m/o is observed to be nearly two orders of magnitude with respect to pure mixed system in the extrinsic conduction region. The enhancement of conductivity in these systems is explained by using Maier's space charge model. The enhancement of conductivity in the dispersed systems is mainly attributed to the increased concentration defects in the space charge layer formed between the host material and the dispersoid. Further, the fall in conductivity may be due to the fall of total effective surface area of contact. The room temperature X-ray diffraction patterns of dispersed systems show the co-existence of three phases. No additional peaks have been noticed in the patterns of dispersed compositions signifies that there is no chemical reaction or formation of solid solution between the host material and dispersoid  $\text{SiO}_2$ . The Fourier Transform Infrared spectrum of dispersed systems in the wave number range from 400 to 4000  $\text{cm}^{-1}$  show the existence of three phases and also confirms the existence of  $\text{OH}^-$  band. The band observed at 835  $\text{cm}^{-1}$  is due to the vibration of N in and out of  $\text{NO}_3$  plane and the strongest absorption at 1385  $\text{cm}^{-1}$  due to asymmetric  $\text{NO}_3$  stretch which confirms the presence of nitrate. The weak absorption which is observed at 735  $\text{cm}^{-1}$  gives the doubly generate O-N-O bending. DSC curves of the pure mixed system and dispersed systems of different m/o of  $\text{SiO}_2$  systems exhibit one endothermic peak due to the only transition that a pure  $\text{NaNO}_3$  has at 272°C and another peak at 299 °C pertains to the melting point of pure mixed system. As observed from the DSC curves, the  $\text{SiO}_2$  content appears to have not affected the transition and melting temperature.

## ACKNOWLEDGEMENTS

The author would like thank the Head, Department of Physics, Osmania University, Hyderabad for extending the experimental facility.

## REFERENCES

1. Chandra S, Superionic Solids; Principles and Applications, Amsterdam, North-Holland,1981.
2. Owens B B and Argue GR. High-Conductivity Solid Electrolytes:  $\text{Mg}_4\text{I}_5$ . Science. 1967;157; 308-310.
3. Bradley JN, Green PD. Solids with high ionic conductivity in group 1 halide systems. Trans Fared Soc. 1967; 63; 424-430.
4. Yao YF, Kummer JT. Ion exchange properties of and rates of ionic diffusion in beta-alumina. J Inorg Nucl Chem. 1967; 29 (9); 2453-2475.
5. West AR. Ionic Conductivity of Oxides based on  $\text{Li}_4\text{SiO}_4$ . J Appl Electrochem. 1973; 3; 327-335.
6. Gracia A, Torres-Trevino G, West AR. New lithium ion conductors based on the  $\gamma\text{-LiAlO}_2$  structure. Solid State Ionics. 1990; 40/41; 13-17.
7. Roth WL, Farrington GC. Lithium-Sodium Beta Alumina: First of a Family of Co-ionic Conductors?. Science. 1977; 196(4296);1332-1334.
8. Reau JM, Magniez G, Rabardel L, Chaminade JP, Pouchard M. Etude de la conductivite ionique dans le tantalate de lithium  $\text{LiTa}_3\text{O}_8\beta$ . Mater Res Bull. 1976; 11(7); 867-871.
9. Angell C A, High conductivity solid ionic conductors (ed.) Takahashi (Singapore: World Scientific),1989.
10. Souquet J L and Kone A, Chowdari B V R and Radhakrishna S (eds), Materials for solidstate batteries Singapore: World Scientific, 1986.
11. Souquet J L, Bruce P G(eds), Solid state electrochemistry, New York: Cambridge Univ. Press, 1995.
12. Tonge J S and Shriver D F (eds), Polymer for electronic applications, CRC Press, 1989.
13. Cowie J M G and Cree S H. Electrolytes Dissolved in Polymers. Annu Rev Phys Chem. 1989; 40; 85-113.

14. Linford R G (eds), *Electrochemical Science and Technology of Polymers 2*, 1990.
15. Bruce P G and Vincent C A. Polymer electrolytes. *J Chem Soc Faraday Trans.* 1993; 89; 3187-3203.
16. Liang CC. Conduction Characteristics of the Lithium Iodide-Aluminum Oxide Solid Electrolytes. *J Electrochem Soc Electrochem Sci Tech.* 1973;120(10);1289-1292.
17. Jow T, Wagner JB. The Effect of Dispersed Alumina Particles on the Electrical Conductivity of Cuprous Chloride. *Jr Electrochem Soc Solid State Sci Tech.* 1979; 126; 1963-1972.
18. Maier J. Heterogeneous Doping of Silver Bromide  $\text{AgBr}:\text{Al}_2\text{O}_3$ . *Mat Res Bull.* 1985; 20; 383-392.
19. Narender Reddy S, Sadananda Chary A, Saibabu K, Chiranjivi T. Enhancement of dc ionic conductivity in dispersed solid electrolyte system -  $\text{Sr}(\text{NO}_3)_2:\gamma\text{-Al}_2\text{O}_3$ . *Solid State Ionics.* 1989; 34(1-2);73-77.
20. Haering C, Roosen A, Schichl H. Degradation of the electrical conductivity in stabilised zirconia systems: Part I: yttria-stabilised zirconia. *Solid State Ionics.* 2005; 176, 3-4 ; 253- 256.
21. Lei Zhao, Yuxia Wang, Zheng Chen, Youming Zou. Preparation, characterization and optical properties of host-guest nanocomposite material SBA-15/AgI. *Physica B.* 2008; 403(10-11); 1775-1780.
22. Kumar A, Shahi K. Conduction mechanism in composite solid state electrolytes:  $\text{PbX}_2$  (X=Cl, Br, I) systems. *J Mater Sci.* 1995;30;4407-4416.
23. Hariharan K, Maier J. Enhancement of the Fluoride Vacancy Conduction in  $\text{PbF}_2:\text{SiO}_2$  and  $\text{PbF}_2:\text{Al}_2\text{O}_3$  Composites. *J Electrochem Soc.*1995;142(10);3469-3473.
24. Foil A Miller, Charles H. Infrared Spectra and Characteristic Frequencies of Inorganic Ions. 1952; 24 (8); 1255-1256.
25. Greenberg J and Hallgren L J. Infrared Absorption Spectra of Alkali Metal Nitrates and Nitrites above and below the Melting Point. *J Chem Phys.* 1960; 33(3); 900-902.
26. Xiaoyi Shen, Yuchun Zhai, Yang Sun and Huimin Gu. Preparation of Monodisperse Spherical  $\text{SiO}_2$  by Microwave Hydrothermal Method and Kinetics of Dehydrated Hydroxyl. *J Mater Sci Technol.* 2010;26(8); 711-714.
27. Madhava Rao MV, Narender Reddy S, Sadananda Chary A. DC ionic conductivity of  $\text{NaNO}_3:\gamma\text{-Al}_2\text{O}_3$  composite solid electrolyte system. *Physica B.* 2005; 362(1-4); 193-198.
28. Vaidehi N, Akila R, Shukla A K, Jacob K T. Enhanced ionic conduction in dispersed solid electrolyte systems:  $\text{CaF}_2\text{-Al}_2\text{O}_3$  and  $\text{CaF}_2\text{-CeO}_2$ . *Mater Res Bull.* 1986; 21; 909.
29. Maier J. Ionic Conduction in Space Charge Regions. *Prog Solid State Chem.* 1995; 23; 171-176.
30. Madhava Rao MV, Narender Reddy S, Sadananda Chary A. Enhancement of DC ionic conductivity in dispersed solid electrolyte system:  $\text{CsNO}_3:\gamma\text{-Al}_2\text{O}_3$ . *Physica B.* 2007; 389;292-295.
31. Reddy S N, Chary A S, Saibabu K, Chiranjivi T. Enhancement of dc ionic conductivity in dispersed solid electrolyte system -  $\text{Sr}(\text{NO}_3)_2:\gamma\text{-Al}_2\text{O}_3$ . *Solid State Ionics.* 1989;34(1-2);73-77.